J|A|C|S ARTICLES

Published on Web 02/03/2010

Silicon Nanosheets and Their Self-Assembled Regular Stacking Structure

Hirotaka Okamoto,*,† Yoko Kumai,† Yusuke Sugiyama,† Takuya Mitsuoka,† Koji Nakanishi,‡ Toshiaki Ohta,‡ Hiroshi Nozaki,† Satoshi Yamaguchi,† Soichi Shirai,† and Hideyuki Nakano†

Toyota Central R&D Laboratories, Inc., Nagakute, Aichi 480-1192, Japan, and The SR Center, Ritsumeikan University, 1-1-1 Noji-Higashi, Kusatsu, Shiga 525-8577, Japan

Received October 16, 2009; E-mail: h-okamoto@mosk.tytlabs.co.jp

Abstract: Silicon nanomaterials are encouraging candidates for application to photonic, electronic, or biosensing devices, due to their size-quantization effects. Two-dimensional silicon nanosheets could help to realize a widespread quantum field, because of their nanoscale thickness and microscale area. However, there has been no example of a successful synthesis of two-dimensional silicon nanomaterials with large lateral size and oxygen-free surfaces. Here we report that oxygen-free silicon nanosheets covered with organic groups can be obtained by exfoliation of layered polysilane as a result of reaction with *n*-decylamine and dissolution in an organic solvent. The amine residues are covalently bound to the Si(111) planes. It is estimated that there is ca. 0.7 mol of residue per mole of Si atoms in the reaction product. The amine-modified layered polysilane can dissolve in chloroform and exfoliate into nanosheets that are 1−2 μm wide in the lateral direction and with thicknesses on the order of nanometers. The nanosheets have very flat and smooth surfaces due to dense coverage of *n*-decylamine, and they are easily self-assembled in a concentrated state to form a regularly stacked structure. The nanosheets could be useful as building blocks to create various composite materials.

Introduction

Nanosheets are two-dimensional nanomaterials that are characterized by a thickness on the order of nanometers and lateral dimensions of submicro- to micrometers. Nanosheets are expected to bridge the gap between the quantum world of zero- or one-dimensional nanomaterials and three-dimensional macroscale bulk materials. The most important feature of nanosheets is their exceptionally high specific surface area, which renders them as promising candidates for a variety of applications, especially in photocatalysis and electrodes of electrochemical devices.[1−3] Many types of nanosheets that consist of oxidized substrates such as silicate layers or metal oxides have been obtained,[1−4] but there have been few reports on the synthesis of two-dimensional silicon nanomaterials.

The reaction of trihalosilane with alkali metal was thought to be a plausible build-up method for the synthesis of silicon nanosheets. Bianconi et al.[5,6] and Matsumoto et al.[7] investigated this reaction and revealed that the reaction products were amorphous bridged polysilane and/or silicon clusters. With this method it is therefore very difficult to control the structural conformation of the products. On the other hand, our group has attempted the synthesis of two types of silicon nanosheets by an exfoliation method. One is a siloxene nanosheet[8] and the other is a Mg-doped silicon nanosheet.[9] Layered siloxene [composition $Si_6H_3(OH)_3$][10] was successfully exfoliated using sodium dodecyl sulfate, although the silicon skeleton was partially oxidized. The Mg-doped silicon nanosheet was prepared through the chemical exfoliation of Mg-doped calcium disilicide (mixed composition $CaSi_{1.85}Mg_{0.15}$), in which the nanosheet maintained the two-dimensional silicon backbone; however, the overall surface of the sheet was capped by oxygen atoms. This oxygen capping is inherent to the process, because the capping is thought to promote exfoliation when the layered silicon becomes a stable colloidal suspension by reaction with aqueous propylamine solution. Thus, oxygen-free silicon nanosheets have not been obtained to date.

In the past decade or so, several silicon-based nanoscale materials, such as nanotubes,[11] nanowires,[12] and nanoparticles,[13]

† Toyota Central R&D Laboratories, Inc.
‡ Ritsumeikan University.

(1) Schaak, R. E.; Mallouk, T. E. *Chem. Mater.* **2002**, *14*, 1455–1471.
(2) Sasaki, T. *J. Ceram. Soc. Jpn.* **2007**, *115*, 9–16.
(3) Kai, K.; Yoshida, Y.; Kageyama, H.; Saito, G.; Ishigaki, T.; Furukawa, Y.; Kawamata, J. *J. Am. Chem. Soc.* **2008**, *130*, 15938–15943.
(4) Tae, E. L.; Lee, K. E.; Jeong, J. S.; Yoon, K. B. *J. Am. Chem. Soc.* **2008**, *130*, 6534–6543.
(5) Bianconi, P. A.; Weidman, T. W. *J. Am. Chem. Soc.* **1988**, *110*, 2342–2344.
(6) Bianconi, P. A.; Schilling, F. C.; Weidman, T. W. *Macromolecules* **1989**, *22*, 1697–1704.
(7) Matsumoto, H.; Miyamoto, H.; Kojima, N.; Nagai, Y. *J. Chem. Soc., Chem. Commun.* **1987**, 1316–1317.
(8) Nakano, H.; Ishii, M.; Nakamura, H. *Chem. Commun.* **2005**, 2945–2947.
(9) Nakano, H.; Mitsuoka, T.; Harada, M.; Horibuchi, K.; Nozaki, H.; Takahashi, N.; Nonaka, T.; Seno, Y.; Nakamura, H. *Angew. Chem., Int. Ed.* **2006**, *45*, 6303–6306.
(10) Weiss, A.; Beil, G.; Meyer, H. *Z. Naturforsch.* **1979**, *34b*, 25–30.
(11) (a) Sha, J.; Niu, J.; Ma, X.; Xu, J.; Zhang, X.; Yang, Q.; Yang, D. *Adv. Mater.* **2002**, *14*, 1219–1221. (b) Park, M.-H.; Kim, M. G.; Joo, J.; Kim, K.; Kim, J.; Ahn, S.; Cui, Y.; Cho, J. *Nano Lett.* **2009**, *9*, 3844–3847.

 10.1021/ja908827z

have been synthesized and have attracted attention due to their remarkable electronic and optical properties. Among many potential applications, silicon nanomaterials are expected to be applied as lithium ion battery anode materials to increase the energy density. Silicon is known to form lithium alloys, and when Li−Si alloys are electrochemically formed the maximum theoretical capacity is approximately 4200 mA h/g, which is much higher than that of the conventionally employed carbonaceous materials (372 mA h/g).[14−16] However, the silicon anode suffers from a large volume change during charge−discharge, which leads to cracking and pulverization of the silicon particles, resulting in drastic capacity fade. A composite involving silicon nanomaterials is a plausible solution to this problem, by minimizing dimensional changes and pulverization failure of Li alloy electrodes during cycling.[15−17] A silicon nanosheet would be the best candidate for an anode material, because of its dimensional features. The large specific area allows effective use of the limited space, contributing to a high energy density, and the effect is emphasized by construction of a stacking structure. Capping of layered silicon compounds with organic groups rather than oxygen atoms is supposed to not only promote their exfoliation, but also assist in the control of the interlayer structure as reconstruction of the stacking structure. Moreover, carbon-coated silicon nanosheets would be obtained by nonoxidative pyrolysis of organically modified nanosheets.

Layered polysilane, Si_6H_6, is a suitable starting material for the preparation of nonoxidative silicon nanosheet by organic modification and exfoliation. Si_6H_6 can be prepared from calcium disilicide ($CaSi_2$),[18,19] and each layer of Si_6H_6 consists of two-dimensional corrugated Si(111) planes, in which the Si_6 rings are interconnected and a H atom is bound to each Si atom in the direction perpendicular to the layer.[10,18,20] With respect to the organic surface modification of silicon particles or substrates, hydrosilylation of hydrogen-terminated silicon surface with unsaturated organic groups such as alkenes and alkynes would be the most applicable method.[21−23] Unfortunately, this reaction hardly proceeded for Si_6H_6 in our preliminary experiments, and a silicon nanosheet could not be obtained. Therefore, another method for the organic modification of Si_6H_6 was required. It is known that ammonia can be dissociatively adsorbed on a Si surface and react with dangling bond sites without major disruption of the Si surface structure.[24] Bergerson et al. and Rogozhina et al. have shown the reaction of *n*-alkylamines on a chlorinated Si surface that was converted from a hydrogen-terminated surface.[25,26] Recently, Liao and Roberts proposed a scheme for irreversible 1-hexylamine adsorption on a hydrogenated Si nanoparticle, in which Si−N bonds were formed.[27] Therefore, reaction between amines and two-dimensional Si layers is worthy of investigation.

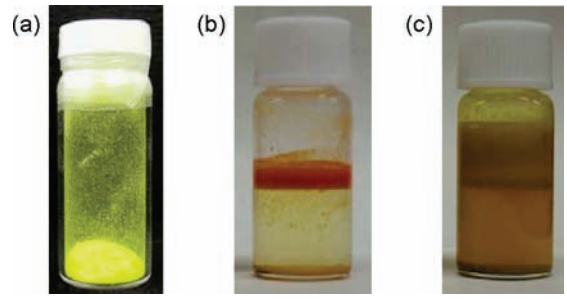

Figure 1. Photographs of material and prepared samples: (a) layered polysilane (Si_6H_6), (b) Si_6H_6 reacted with *n*-decylamine (C10−Si_n) for 12 h in chloroform at 60 °C in a nitrogen atmosphere, and (c) C10−Si_n after heating at 120 °C for ca. 24 h.

Here we report an approach to the synthesis of oxygen-free silicon nanosheets covered with amines using Si_6H_6 as a starting material and the structural characterization of the resulting nanosheets and their self-assembled stacking structures.

Results and Discussion

Reaction of Si_6H_6 with *n*-Decylamine. Si_6H_6 is a yellow-colored powder (Figure 1a) and precipitates in chloroform or other organic solvents. The color of Si_6H_6 changed to orange after stirring in a mixture of *n*-decylamine and chloroform for approximately 1 h at 60 °C in a nitrogen atmosphere. Most of the orange-colored powder floated on the chloroform surface after 12 h of stirring (Figure 1b). There were no precipitates except for a trace amount of white and black precipitates, which were silica and reduced crystal silicon. The floatation of the powder suggests that the density of Si_6H_6 becomes lower than that of chloroform due to attachment of *n*-decylamine. A large amount of the powder could be uniformly dispersed in chloroform and the solution became turbid after further heat treatment without chloroform (Figure 1c). These results suggest that the organic surface modification of silicon layers is successfully achieved by the reaction of Si_6H_6 with *n*-decylamine, and the product was obtained in more than 90% yield.

The orange color change of Si_6H_6 also progressed without heating but required a much longer time, which suggests that heating promotes the modification of Si_6H_6. In contrast, a similar treatment without chloroform leads to a different result. When *n*-decylamine was poured onto Si_6H_6, bubbles were formed on Si_6H_6, but further observable change did not occur for some time afterward, even if *n*-decylamine and Si_6H_6 was kept stirred at 120 °C. The color of Si_6H_6 was slightly dulled and the powder swelled somewhat after a few days of stirring; the swollen powder could float and disperse when it was put in chloroform,

(12) (a) Morales, A. M.; Lieber, C. M. *Science* **1998**, *279*, 208–211. (b) Cui, Y.; Zhong, Z.; Wang, D.; Wang, W. U.; Lieber, C. M. *Nano Lett.* **2003**, *3*, 149–152.
(13) (a) Tilley, R. D.; Warner, J. H.; Yamamoto, K.; Matsui, I.; Fujimori, H. *Chem. Commun.* **2005**, 1833–1835. (b) Bley, R. A.; Kauzlarich, S. M. *J. Am. Chem. Soc.* **1996**, *118*, 12461–12462.
(14) Sharma, R. A.; Seefurth, R. N. *J. Electrochem. Soc.* **1976**, *123*, 1763–1768.
(15) Komaba, S.; Mikami, F.; Itabashi, T.; Baba, M.; Ueno, T.; Kumagai, N. *Bull. Chem. Soc. Jpn.* **2006**, *79*, 154–162.
(16) Yoshio, M.; Wang, H.; Fukuda, K.; Umeno, T.; Dimov, N.; Ogumi, Z. *J. Electrochem. Soc.* **2002**, *149*, A1598–A1603.
(17) Besenhard, J. O.; Yang, J.; Winter, M. *J. Power Sources* **1997**, *68*, 87–90.
(18) Yamanaka, S.; Matsu-ura, H.; Ishikawa, M. *Mater. Res. Bull.* **1996**, *31*, 307–316.
(19) Nishimura, K.; Nagao, Y.; Yamanaka, S.; Matsu-ura, H. *Jpn. J. Appl. Phys.* **1996**, *35*, L293–L296.
(20) Dahn, J. R.; Way, B. M.; Fuller, E.; Tse, J. S. *Phys. Rev. B* **1993**, *48*, 17872–17877.
(21) Linford, M. R.; Chidsey, C. E. D. *J. Am. Chem. Soc.* **1993**, *115*, 12631–12632.
(22) Linford, M. R.; Fenter, P.; Eisenberger, P. M.; Chidsey, C. E. D. *J. Am. Chem. Soc.* **1995**, *117*, 3145–3155.
(23) Effenberger, F.; Götz, G.; Bidlingmaier, B.; Wezstein, M. *Angew. Chem., Int. Ed.* **1998**, *37*, 2462–2464.
(24) Waltenburg, H. N.; Yates, J. T., Jr. *Chem. Rev.* **1995**, *95*, 1589–1673.
(25) Bergerson, W. F.; Mulder, J. A.; Hsung, R. P.; Zhu, X.-Y. *J. Am. Chem. Soc.* **1999**, *121*, 454–455.
(26) Rogozhina, E.; Belomoin, G.; Smith, A.; Abuhassan, L.; Barry, N.; Akcakir, O.; Braun, P. V.; Nayfeh, M. H. *Appl. Phys. Lett.* **2001**, *78*, 3711–3713.
(27) Liao, Y.-C.; Roberts, J. T. *J. Am. Chem. Soc.* **2006**, *128*, 9061–9065.

Scheme 1. Proposed Reaction Scheme for the Production of C10−Si_n from Si_6H_6 and *n*-Decylamine

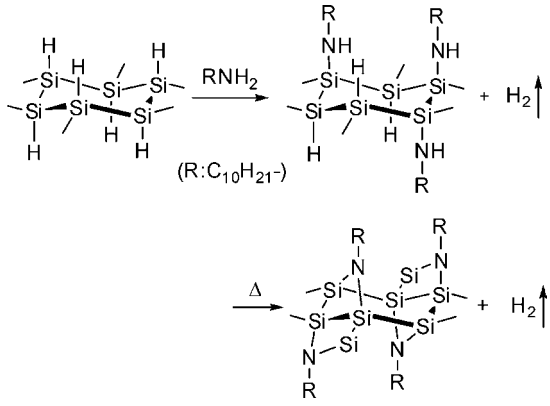

which indicates that the addition of chloroform is advantageous for the modification.

A similar change was observed when *n*-butylamine was used instead of *n*-decylamine. On the other hand, there were no significant changes after stirring with di-*n*-butylamine or tri-*n*-butylamine for 12 h at 60 °C, although some modification was achieved in the former case after 60 h of heat treatment at 120 °C. These samples precipitated and did not disperse in chloroform, even after heat treatment. When aniline was used as a modifier, no considerable changes were observed just after stirring in chloroform. However, a small amount of surface-modified Si layers were obtained, which were homogeneously dispersed in chloroform following heat treatment.

There are two possible outcomes concerning the binding mode in this surface modification; the amine reacts with Si_6H_6 or it attaches to the surface of the silicon layers. In the case of reaction, the following scheme is considered (Scheme 1). Some Si−H bonds on Si_6H_6 react with amine molecules to form Si−NH−R linkages (R = decyl group). The N−H bond in the Si−NH−R linkages reacts with another Si−H bond on Si_6H_6 to form a Si−NR−Si linkage, and hydrogen gas is released at each step. The final product is thought to contain both Si−NH−R and Si−NR−Si linkages in variable proportions, depending on the reaction conditions.

Bubble formation observed just after pouring the amine onto Si_6H_6 implies that hydrogen is generated as a result of the reaction. The first evidence for reaction was obtained using Fourier transfer infrared spectroscopy (FTIR) (Figure 2). The FTIR spectrum of the obtained sample shows strong C−H stretching vibrations in the wavenumber range from 2800 to 3000 cm^{-1} and weak C−H bending vibrations from 1350 to 1450 cm^{-1}. These vibrations are attributed to the alkyl chain of *n*-decylamine, which indicates that the *n*-decylamine residue is included in the reaction product. The sample does not exhibit a peak around 2100 cm^{-1}, indicating Si−H stretching vibrations, as observed for Si_6H_6. Moreover, there is no broad peak around 3300 cm^{-1}, which is assignable to N−H stretching, as observed for *n*-decylamine. On the other hand, a weak peak at 930 cm^{-1} is observed in this sample, which is assigned to asymmetric Si−N−Si stretching.[28] These results indicate that *n*-decylamine is not merely attached to Si_6H_6 but reacts with Si_6H_6. The broad peak around 3300 cm^{-1} for Si_6H_6 still remained for the sample treated without chloroform with a slight shift to lower wave-

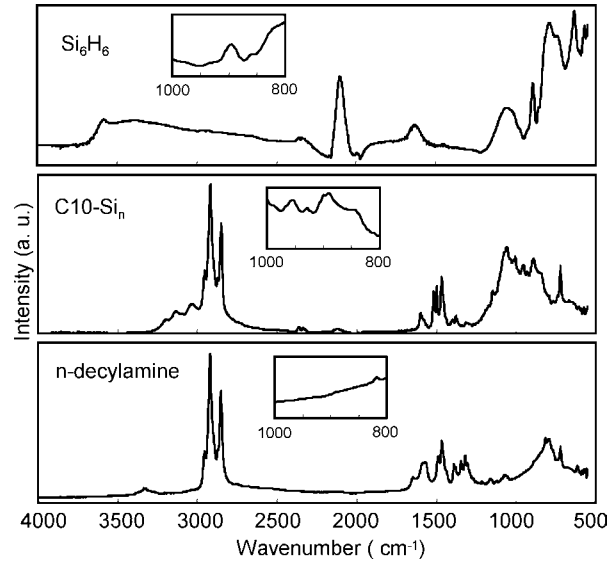

Figure 2. FTIR spectra of Si_6H_6, *n*-decylamine, and C10−Si_n. The insets show enlarged spectra in the range from 800 to 1000 cm^{-1}.

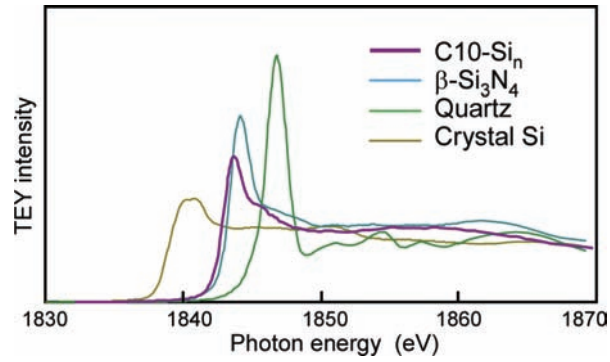

Figure 3. Comparison of XANES spectra of C10−Si_n with those of quartz, crystal silicon, and β-Si_3N_4 obtained using the TEY mode in a vacuum.

number, although the peak around 2100 cm^{-1} disappeared. In contrast, the latter peak remained in the precipitates of Si_6H_6 after stirring with di-*n*-butylamine or tri-*n*-butylamine.

Si K-edge X-ray absorption near-edge structure (XANES) also revealed a Si−N linkage in the layered polysilane that was reacted with *n*-decylamine (C10−Si_n) (Figure 3), with a large peak around 1844 eV detected using the total electron yield (TEY) method. This peak is very close to that observed for β-silicon nitride measured as a reference sample and is different from those peaks observed for crystalline silicon, quartz, siloxene, or layered polysilane,[20] which suggests that C10−Si_n contains Si−N linkages and no Si−O linkages.

After confirmation of Si−N linkages that connect amine residues to Si layers, it is necessary to check the validity of the reaction proposed in Scheme 1. There is the possibility that the first step to form Si−NH−R linkage must not be dependent on the stability of the reaction product but depend on the reactivity between amines and Si_6H_6, because a Si−NH−R linkage does not cause any energetic disadvantage such as structural distortion. The Si−H bond in Si_6H_6 is assumed to be silyl hydride (i.e., the Si atom is cationic and the H atom is anionic), so that Si atoms can easily accept the attack of a lone electron pair from a N atom in the amine. The H atom of the Si−H bond then combines with that of the amine N−H bond and they are eliminated as H_2 gas. In previous reports, a chlorinated Si(100)

(28) Socrates, G. *Infrared and Raman Characteristic Group Frequencies; Table and Charts*, 3rd ed.; Wiley: New York, 2001.

surface, porous silicon, and Si particle have been successfully reacted with *n*-alkylamines or aniline to form Si−N linkages.[25,26] These studies required the conversion of the Si−H bond to a Si−Cl bond to form a Si−N linkage. Recently, hydrogenated Si nanoparticles have also been reacted with *n*-hexylamine to form Si−N linkages.[27] With regard to reactivity with *n*-alkylamines, Si−H bonds on two-dimensional silicon layers are thought to be more reactive than those on bulk Si silicon and equal to those on Si nanoparticles. Nevertheless, the color change does not proceed so fast, but heating for a long time is required to achieve a good dispersion in chloroform. It is conjectured that the migration of *n*-decylamine into the space between silicon layers controls the total reaction rate; the reaction proceeds promptly on the surface of Si_6H_6 agglomerates but is slow in the interlayer space due to slow insertion of *n*-decylamine molecules. Heating and the addition of chloroform are expected to promote the migration of amine molecules and hence the reaction. The lower nucleophilicity of di-*n*-butylamine, tri-*n*-butylamine, and aniline than *n*-decylamine and *n*-butylamine should result in lower reactivity. It is thought that the sterically bulky structures of the former two butylamines also dampens the reaction rate due to slower insertion into the interlayer space. Moreover, reaction with tri-*n*-butylamine does not proceed at all, because no H_2 elimination occurs after nucleophilic attack of the amine.

The second step of Scheme 1 is supposed to be formed by the reaction between alternately adjacent Si−NH−R and Si−H, in the same manner as the first step. The structural stability of the reaction product must strongly affect the feasibility of the reaction, because the Si−NR−Si bridge induces severe distortion in the silicon layer. The formation of Si−N−Si linkages was proposed by Bergerson et al.[25] and Liao and Roberts[27] but doubted by Rogozhina et al.[26] In the case of dissociative adsorption of ammonia on a bulk Si surface, a stable Si−NH−Si linkage was formed not on Si(100)-(2 × 1), but on Si(111)-(7 × 7) by heating from 300 to 600 K. Si(111)-(7 × 7) has a strained Si adatom backbone, which was broken as −NH− was inserted into the backbone.[29] However, Si_6H_6 is thought to consists of Si(111)-(2 × 1), which does not include any distortion, and hence, the above mechanism cannot be applicable. If a Si−N−Si bridge was introduced on two-dimensional Si(111)-(2 × 1) and optimized, then the sheet would warp, as shown in Figure 4a. This structure would contradict the flat nanosheet and regularly stacked multilayers, as shown later. Many bridges would cause even more sever warping or a less-stable state. However, if two Si−N−Si bridges are introduced on both sides of the six-membered ring in the sheet, a symmetric flat sheet could be obtained (Figure 4b). This bridge formation on both sides is achievable for each Si_6H_6 sheet but is not available for bulk Si surfaces. The two-dimensional Si structure allows a flat sheet conformation with the Si−N−Si bridge and, hence, is thought to cause different reactivity from that of the bulk surface. Warpage or instability may be induced even if this bridge is formed on the Si(100)-(2 × 1) surface, because the stable Si−Si bond length (0.235 nm) is shorter than the distance between Si atoms in a fully relaxed Si−N−Si molecular complex (0.31 nm).[24,29]

It is assumed that the formation of two Si−NH−R linkages would be energetically favorable compared with that of one Si−N−Si bridge, in terms of structural distortion. However, not all Si−H bonds could be replaced by Si−NH−R bonds, due to the bulkiness of the long alkyl chains in the amine residues. According to molecular modeling of octadecyl monolayers on the Si(111) surface, not more than 50% of alkyl chains can substitute to Si dangling bonds.[30] Therefore, Si−H bonds left among Si−NH−R bonds react with surrounding amine residues instead of new amine molecules, so that Si−N−Si bridges would be formed.

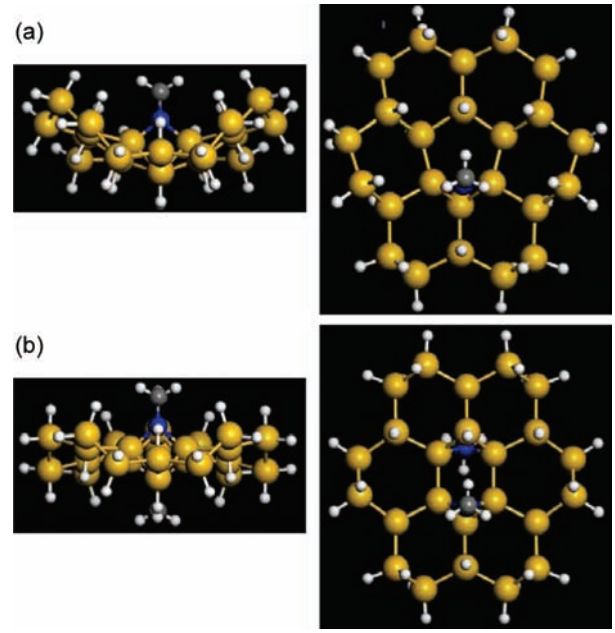

Figure 4. Side (left) and top (right) views of the energetically optimized structure of a part of a Si(111)-(2 × 1) monolayer with methylamine residue(s) that form −NR− bridge(s) between alternately adjacent Si atoms. Monolayer with (a) a single bridge and (b) double bridges on both sides. Methylamine was used instead of *n*-decylamine to simplify the calculation.

It is noteworthy that organic modification of Si_6H_6 with alkenes and alkynes is difficult to achieve by hydrosilylation. It is speculated that Si radicals generated as reaction intermediates are not stable, so that Si−H bond dissociation would not be induced by heating or UV irradiation. The organic modification of Si_6H_6 by reaction with amine presented here is a much better pathway than hydrosilylation.

The amine-modified Si_6H_6 is oxidized in air but is thermally stable. The thermal stability of C10−Si_n and the amounts of *n*-decylamine bound to the silicon layers were investigated using thermogravimetric analysis (TGA). The TGA curve of C10−Si_n is shown in Figure 5. C10−Si_n begins to lose weight above 80 °C and the loss continues up to approximately 510 °C. There are three inflection points at 165, 257, and 314 °C. The weight loss below 165 °C is thought to be due to detachment of *n*-decylamine that attaches or weakly binds to the silicon sheets, from a comparison of the TGA curve of *n*-decylamine. The 70% weight loss in the temperature range from 165 to 510 °C must be accounted for by the loss of *n*-decylamine bound to the sheets. Remaining alkyl chains were confirmed by FTIR for the sample measured up to 400 °C. The fragments above 510 °C are considered to be silicon layers. The presence of remnant alkyl chains at over 500 °C indicates the high thermal stability of C10−Si_n. This stability is consistent with the results of the combination of *n*-octylamine and the Si(100) surface.[25] The

(29) Chen, P. J.; Colaianni, M. L.; Yates, J. T., Jr. *Surf. Sci.* **1992**, *274*, L605–L610.

(30) Sieval, A. B.; van den Hout, B.; Zuilhof, H.; Sudhölter, E. J. R. *Langmuir* **2000**, *16*, 2987–2990.

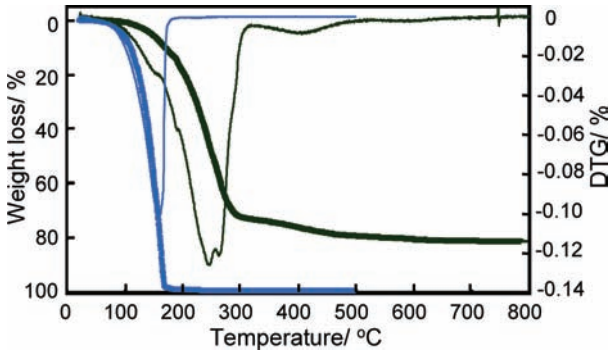

Figure 5. TGA curves (thick lines) of C10−Si_n (green line) and *n*-decylamine (blue line) under nitrogen flow. The temperatures of weight loss are indicated in the corresponding differential thermogravimetric (DTG) curves (thin lines).

presence of ca. 0.7 mol of *n*-decylamine residue per mole of Si atoms is estimated in C10−Si_n, based on the weights of the bound amine residue and silicon atom. If all *n*-decylamine residues were bound to the silicon sheet through Si−NR−Si linkages, the maximum estimated value would be 0.5 mol of *n*-decylamine residue. A portion of the *n*-decylamine residues are thought to bind with the sheet through Si−NH−R linkages. Even if the estimation is slightly ambiguous, it is evident that the silicon sheet is densely covered with *n*-decylamine residues and has few defects.

Structure and Spectrophotometric Characteristics of the Nanosheet. The C10−Si_n nanosheet structure was observed using atomic force microscopy (AFM). A sample was prepared by dropping a dilute solution of C10−Si_n (0.01%) in chloroform onto a highly oriented pyrolytic graphite (HOPG) plate, followed by volatilization of the solvent. A two-dimensional sheet structure with lateral dimensions in the range of 1−2 μm was observed (Figure 6a). The thickness of the sheets was measured at the intervals between the sheets and at the substrate surface to yield a mean value of 7.5 nm (Figure 6b). The AFM image also reveals that the nanosheet has a very flat and smooth surface, which is due to the dense coverage of *n*-decylamine, as expected from the TGA result. The thickness of this nanosheet is 10 times larger than that of a siloxene nanosheet[8] or 20 times larger than that of a Mg-doped silicon nanosheet.[9] These differences are not surprising, because long alkyl chains are connected to the surface of the C10−Si_n nanosheet on both sides, while the dangling bonds of the siloxene bind with a combination of hydroxyl groups and hydrogen atoms or those of Mg-doped silicon nanosheets do with oxygen atoms. The value of 7.5 nm corresponds to the thickness of two to three pieces of the amine-modified silicon monolayers, from comparison with the X-ray diffraction (XRD) results described later. This implies that a completely exfoliated structure has not been observed by AFM. C10−Si_n and other amine-modified nanosheets have a strong tendency to stack when they are extracted from solution by evaporation of the solvent. This property makes it difficult to capture the monolayer structure. The thickness of the observed nanosheet is not equal to the integral multiple of the monolayer thickness. This discrepancy may be due to solvent remaining between the HOPG plate and the nanosheets or their interlayer spaces.

Spectrophotometric measurements of dilute C10−Si_n solutions also reflect characteristics of the nanosheet structure. UV−vis absorption of the nanosheets shows a peak at 276 nm with a shoulder around 283 nm (Figure 7). This peak position

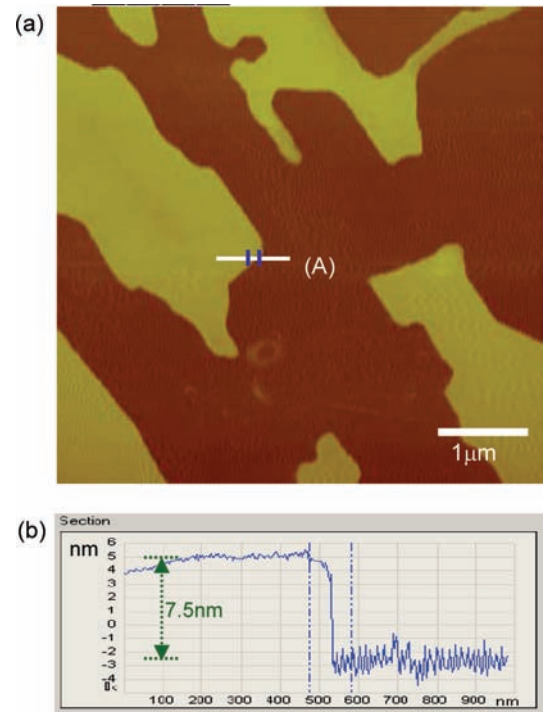

Figure 6. (a) AFM phase image of a C10−Si_n nanosheet on a HOPG plate obtained in tapping mode. (b) Line profile measured along the white line denoted as (A) in panel a.

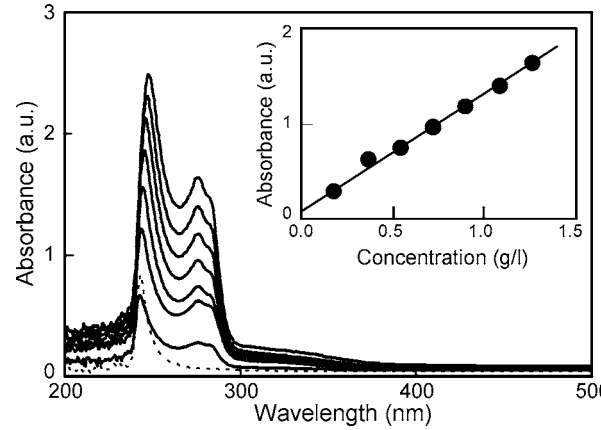

Figure 7. UV−vis spectra of chloroform solutions of silicon nanosheets at various concentrations. The dotted line is the spectrum of *n*-decylamine in chloroform. The inset shows absorbance at 276 nm plotted against the concentration of the nanosheets.

is very close to that for the siloxene nanosheet (ca. 300 nm),[8] the Mg-doped silicon nanosheet (268 nm),[9] and alkyl-terminated silicon nanoclusters ranging from 2 to 5 nm in diameter (ca. 280 nm).[31] Moreover, the absorption edge of the C10−Si_n solution at approximately 380 nm corresponds to that of the nanoclusters (360−390 nm). These peak and edge positions are considerably blue-shifted from the band gap of bulk silicon. The peak intensity is proportional to the concentration of the chloroform solution, and the linear relationship indicates complete dispersion of the nanosheets as monolayers. C10−Si_n solutions have another peak around 243 nm, attributable to *n*-decylamine residues connected to the silicon sheet.

(31) Yang, C. S.; Bley, R. A.; Kauzlarich, S. M.; Lee, H. W. H.; Delgado, G. R. *J. Am. Chem. Soc.* **1999**, *121*, 5191–5195.

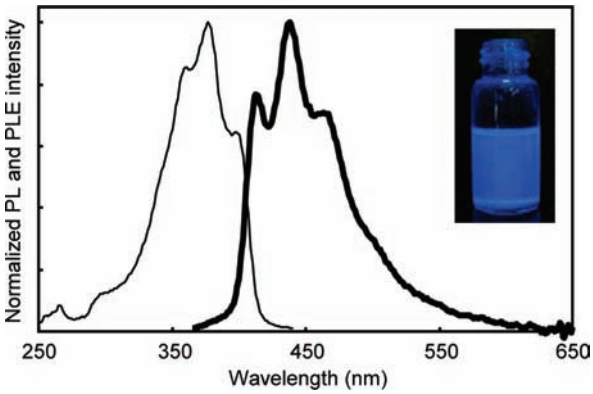

Figure 8. PL (thick line) and PLE (thin line) spectra of C10−Si_n in chloroform. Excitation and fluorescence wavelengths are 350 and 450 nm, respectively. The inset photograph shows the fluorescent emission from a chloroform solution of C10−Si_n exposed to UV with a wavelength of 365 nm.

Blue light emission is observed when the C10−Si_n chloroform solution is exposed to UV light with a wavelength of 365 nm. A broad main peak appears at 438 nm (2.8 eV) in the photoluminescence (PL) spectrum obtained using an excitation wavelength of 350 nm (Figure 8). The peak positions are mostly the same as that for Mg-doped silicon nanosheet[9] or a silicon network polymer with hexyl side chains.[32] Therefore, C10−Si_n shifts slightly to higher energy compared with Si_6H_6, of which the band gap energy was measured as approximately 2.3 eV.[19] The band gap energy of the two-dimensional silicon material was calculated as 2.5 eV, and the dimensionality is thought to play an important role in the band gap energy, in addition to the broadness of the PL spectra.[32] The consistency with these reports supports the existence of the C10−Si_n nanosheet structure. PL and PL emission (PLE) spectra obtained using excitation wavelengths of 450 nm also resemble each other, as shown in Figure 8. It should be noted that the PL is not related to amine itself or a heat-denatured amine, because blue light emission was not observed from a mixture of chloroform and *n*-decylamine either before or after heating.

Regular Stacking Structure of Silicon Nanosheets. Internal structures in the agglomerated state of C10−Si_n and other amine-modified Si nanosheets were detected by XRD. Samples were prepared by dropping solutions of C10−Si_n in chloroform onto a glass plate, followed by volatilization of the solvent. A very strong and narrow peak at $2\theta = 2.96°$, which corresponds to $q = 2.11$ nm^{-1} in the wavenumber vector [$q = (4\pi/\lambda) \sin\theta$] scale, was observed for C10−Si_n (Figure 9a). This peak relates to the interlayer distance ($d = 2.98$ nm) of the nanosheets and appears together with its higher order peaks, which can be assigned as (00*l*) planes. No other peaks were observed. This diffraction characterizes the stacking of the nanosheets. Thus, the nanosheets agglomerate in a concentrated state to form a regularly stacked structure by self-assembly. Although C10−Si_n is oxidized in air, the XRD patterns remained intact and did not disappear easily; therefore, the interior of the agglomerate is assumed to have oxidation resistance and maintains the regularly stacked structure.

The peak derived from the (001) plane is much sharper than that of Si_6H_6 (Figure 9e). The broadness of the latter peak is attributed to the small crystallite size, in which approximately

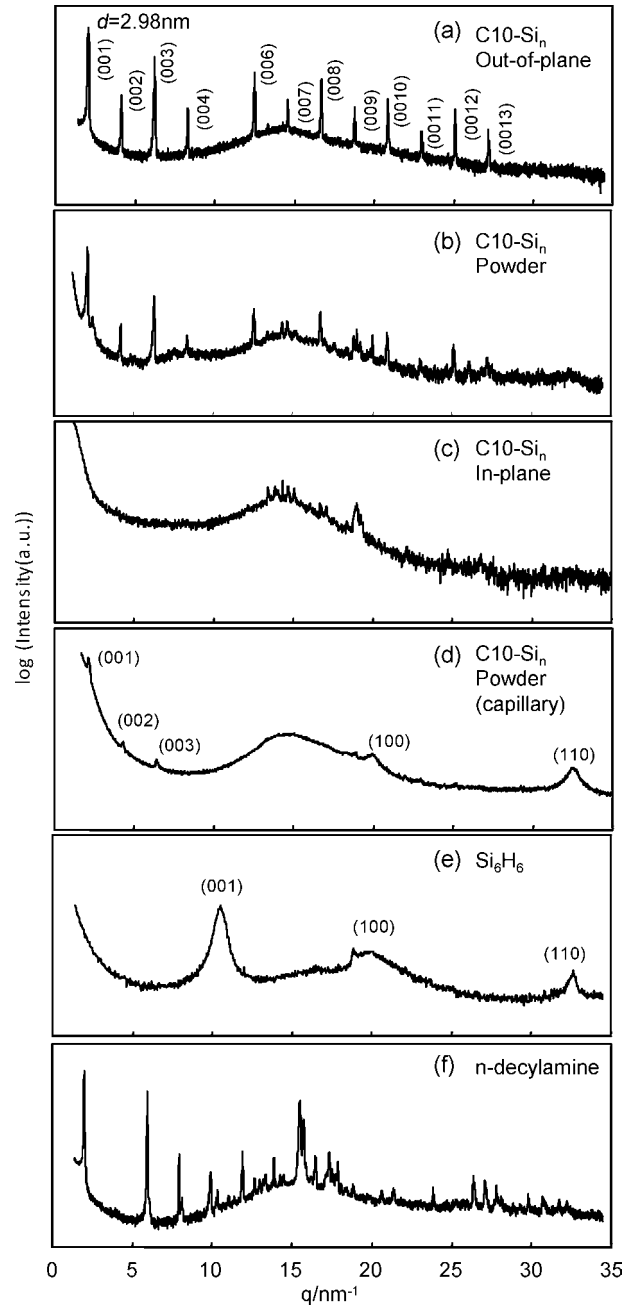

Figure 9. XRD patterns of (a−d) C10−Si_n with (e) Si_6H_6 and (f) *n*-decylamine for comparison. (a) Out-of-plane, (b) powder and (c) in-plane patterns of the C10−Si_n layered sample in which silicon layers are stacked parallel to the surface of the glass plate. (d) Pattern measured using a powder sample filled in a glass capillary. Patterns c and d were measured using synchrotron radiation, and parts of the samples were destroyed during measurements.

10 layers are included.[20] The strong and sharp peak of C10−Si_n also indicates multilayer stacking consisting of more than tens of layers.

Sharp and periodical peak patterns appear for the *n*-butylamine- and aniline-modified samples (Figure 10a,d). Similar stacking structures are thought to be constructed in these samples with interlayer distances estimated as 1.54 and 1.43 nm, respectively. On the other hand, there is no periodical pattern for the di-*n*-butylamine- and tri-*n*-butylamine-modified samples (Figure 10b,c). Peaks that suggest an increment of the Si_6H_6 interlayer distance appear at $2\theta = 3.22°$ and 7.65° for the former

(32) Furukawa, K.; Fujino, M.; Matsumoto, N. *Macromolecules* **1990**, *23*, 3423–3426.

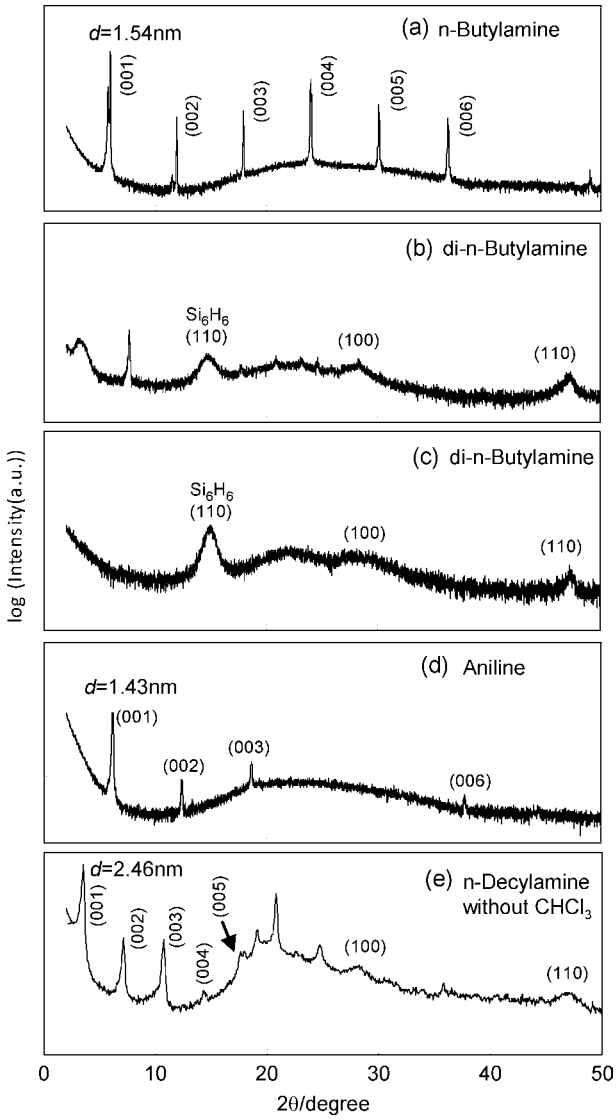

Figure 10. XRD patterns of (a) *n*-butylamine-, (b) di-*n*-butylamine-, (c) tri-*n*-butylamine-, (d) aniline-, and (e) *n*-decylamine-modified Si sheets. The last sample was synthesized without using chloroform in the modification process. XRD samples of a, d, and e were prepared from chloroform solutions, but those of c and d were precipitates in chloroform.

sample, but there is little difference between Si_6H_6 and the latter sample. These results support the presumption that secondary amines have low reactivity to Si_6H_6 and that tertiary amines do not react with Si_6H_6. A different peak pattern from that for C10−Si_n was observed for the *n*-decylamine-modified sample obtained without chloroform in the modification process (Figure 10e). Although periodical peak patterns appear in the lower angle region, the peak corresponding to the (001) plane appears at $2\theta = 3.59°$ ($d = 2.46$ nm). This suggests that the reaction without solvent leads to a different structure in the modified Si sheets.

In contrast to the out-of-plane pattern, several additional peaks appear at $q > 13$ nm^{-1} in the XRD pattern of the C10−Si_n powder sample (Figure 9b). These peaks also appear in the in-plane XRD pattern of the sample used for the out-of-plane measurement (Figure 9c). The peaks are thought to be derived from ordered structures composed of *n*-decylamine residues on silicon layers, although the peak assignment will be investigated in more detail. The alkyl chains in stacked C10−Si_n are supposed to align differently from those in *n*-decylamine crystals

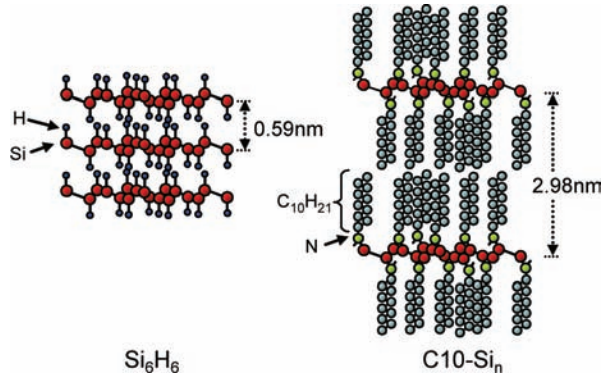

Figure 11. Structural models of Si_6H_6 and regularly stacked C10−Si_n.

(Figure 9f), due to binding to the silicon layers. The value of $d = 2.98$ nm suggests that the *n*-decylamine residues on the corrugated silicon layers are almost perpendicular to the layers with extended chain conformation (Figure 11), because the thickness of the layer is 0.16 nm. Both *n*-butylamine- and aniline-modified Si layers are thought to have similar structures. On the other hand, the alkyl chains in the *n*-decylamine-modified sample prepared by reaction without solvent must not be perpendicular to the layers. It is known that *n*-decylamine can be intercalated into layered siloxene in aqueous emulsion and that the interlayer distance expands from 0.63 to 2.54 nm. Bilayers of alkyl chains with tilted (tilting angle ca. 40°) or coiled chains are assumed to be present in the siloxene interlayers.[10] Similar tilting structures should also be available for the modified C10−Si_n samples, because the interlayer distance is similar ($d = 2.46$ nm). In every case, dense covering and ordered alignment of *n*-decylamine residues is thought to contribute to the highly regular stacking. It is also supposed that the thick alkyl layers weaken the interaction between adjacent Si layers, so that specific structures cannot be constructed in the lateral direction.

The remaining two-dimensional silicon crystal structure was confirmed by XRD measurement of C10−Si_n powder filled into glass capillaries (Figure 9d). Peaks corresponding to the (100) and (110) planes of the corrugated silicon sheet are observed around 20.4 and 32.8 nm^{-1}, respectively. A few peaks corresponding to the (00*l*) planes of C10−Si_n are also observed, although higher order peaks are absent, due to the destruction of the *n*-decylamines residues by synchrotron radiation. The absence of peaks corresponding to the (001) planes of Si_6H_6 and $CaSi_2$ confirms that the peaks of the (100) and (110) planes are derived from the two-dimensional silicon crystals included in C10−Si_n. A broad peak corresponding to the (110) plane also appears in Figure 9b.

The regular microscale stacking structure seems to form noticeable structures, such as jelly- and spongelike agglomerates in the macroscale. A jellylike agglomerate can be formed by dissolving a slightly oversaturated amount of C10−Si_n in toluene and slowly volatilizing the solvent to concentrate the solution. This agglomerate is not a gel in the strict sense, because it does not exhibit elastic recovery under strain. However, it does lose fluidity, as shown in Figure 12a. A spongelike agglomerate was obtained from a slightly oversaturated amount of C10−Si_n in a mixture of toluene and chloroform by slow volatilization of the solvents until fully dried. The residue is a spongelike agglomerate composed of flakes with thicknesses of approximately a few

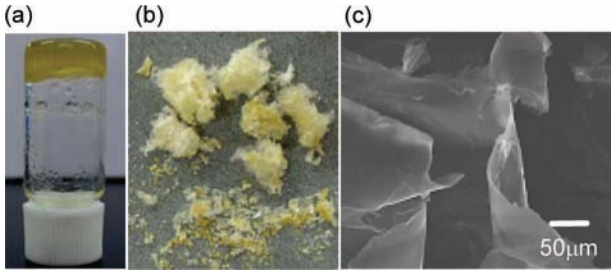

Figure 12. (a) Jellylike agglomerate of C10−Si_n obtained by dissolving a slightly oversaturated amount of C10−Si_n in toluene and slowly volatilizing the solvent to concentrate the solution. (b) Spongelike agglomerate of C10−Si_n obtained by dissolving a slightly oversaturated amount of C10−Si_n in a mixture of toluene and chloroform and slowly volatilizing the solvents to dryness. (c) SEM image of sample b.

hundred nanometers, as shown in Figure 12b,c. Both agglomerates exhibit XRD patterns similar to those shown in Figure 9a.

Conclusion

Oxygen-free silicon nanosheets covered with organic groups were synthesized by exfoliation of layered polysilane as a result of reaction with *n*-decylamine and dissolution in chloroform. The amine residues are covalently bound to the Si(111) planes. It is estimated that there is ca. 0.7 mol of residue per mole of Si atoms in the reaction product. The product can be dissolved in chloroform to obtain nanosheets, which are 1−2 μm wide in the lateral direction with thicknesses on the order of nanometers. The nanosheets are easily self-assembled in a concentrated state to form a regularly stacked structure. The nanosheets would be useful as building blocks for the preparation of various composite materials. The organic modification method presented here is applicable to other primary amines or secondary amines, although perfect exfoliation and regularly stacked structure of the Si layers may not be achieved in the latter case. Amine-modified nanosheets are expected to be applied to optical or electronic devices in the future.

Experimental Section

Materials. $CaSi_2$ was purchased from Soegami Chemical Co. Dehydrated chloroform and toluene, *n*-decylamine *n*-butylamine, di-*n*-butylamine, tri-*n*-butylamine, and aniline were purchased from Wako Pure Chemical Industries, Ltd. The dehydrated chloroform contained a small amount of amylene as a stabilizer to prevent radical cleavage. All reagents were used without further purification.

Sample Preparation. Si_6H_6 was prepared according to the method described by Yamanaka et al.[18,19] Approximately 1 g of selected $CaSi_2$ crystallites with 5 mm^2 faces was immersed in 100 mL of 37% HCl at −30 °C. The mixture was stirred continuously for 5 days under an Ar atmosphere. The synthesized Si_6H_6 was rinsed in dilute HF solution and then dried by evacuation at 110 °C.

The amination of Si_6H_6 was performed in an inert atmosphere; 0.1 g of Si_6H_6 (340 mmol of Si−H unit) was placed into a Schlenk flask with a screw cap in a glovebox. The Schlenk flask was connected to a nitrogen gas line, and then 420 mmol of *n*-decylamine was added with ca. 10 mL of dehydrated chloroform, followed by stirring at 60 °C for 12 h. After evaporation of the chloroform, the reactant was heated at 120 °C for approximately 24 h in a closed vessel. The sample was transferred to a sample tube, into which chloroform was poured to remove the small amount of white and black precipitates, which were confirmed as silica and reduced crystal silicon by infrared spectroscopy. The aminated sample that floated on or dissolved in chloroform was distilled under reduced pressure. After adding fresh chloroform or toluene to the sample, the suspension was redistilled to remove unreacted amine. Distillation for refinement was repeated twice. The same procedure was performed for amines instead of *n*-decylamine. When Si_6H_6 was reacted with *n*-decylamine without chloroform, the mixture was kept stirring at 120 °C for 60 h.

A slightly oversaturated amount of the refined C10−Si_n was dissolved in toluene and a mixture of toluene and chloroform (50/50 v/v). The solvents were slowly evaporated from both solutions under a nitrogen atmosphere. The toluene solutions concentrated to form a jellylike agglomeration, and a spongelike agglomeration was obtained from the mixed solvent solution.

Characterization. Fourier Transfer Infrared Spectroscopy (FT-IR). FT-IR spectra were recorded on a Nicolet FT-IR Avatar360 spectrometer with 4 cm^{-1} resolution. The attenuation total reflection method was used with a small amount of refined sample placed on a diamond substrate. Data sampling was repeated 32 times.

X-ray Absorption Near-Edge Structure (XANES). Si K-edge X-ray absorption spectroscopy was measured at the double crystal monochromator beamline of BL-10 at the Ritsumeikan University SR Center. InSb(111) crystal was used as a monochromator, of which the energy resolution was approximately 1.5 eV at the Si K-edge.

A chloroform solution of nonrefined C10−Si_n was applied to a HOPG plate, dried in air, and then transferred to a chamber filled with helium gas. A silicon drift detector was set in the direction perpendicular to the incident radiation through the sample. Fluorescence yield (FY) mode was employed for measurement of the spectrum. After the measurement, the HOPG plate was transferred to a vacuum chamber with a base pressure in the range of 10^{-5} Pa, and XANES spectra were measured using both total electron yield (TEY) and fluorescence yield (FY) modes.

Thermogravimetric Analysis (TGA). TGA data were obtained with a Rigaku Thermo Plus TG8120 using 5−10 mg of refined sample at a heating rate of 10 °C/min under nitrogen flow.

Atomic Force Microscopy (AFM). AFM samples were prepared by dropping a dilute solution of C10−Si_n (0.01%) in chloroform onto a HOPG plate, followed by volatilization of the solvent. AFM images were obtained with a Veeco NanoScope IV in tapping and contact modes.

Scanning Electron Microscopy (SEM). The spongelike agglomerates were observed using SEM (Hitachi High-Technologies S-3600, operated at 15 kV). The spongelike sample was placed on an aluminum stage and fixed with conductive adhesive tape. The sample was not exposed to further treatment such as gold sputtering of the surface.

X-ray Diffraction (XRD). Powder XRD patterns of the refined samples were obtained using a Rigaku RINT-TTR with Cu Kα radiation generated at 50 kV and 300 mA and a scanning rate of 2°/min. Out-of-plane XRD patterns of the layered sample structure were also obtained using the same equipment under the same conditions. Samples were prepared by dropping a chloroform solution of the refined sample onto a glass plate and drying in air, with the exception of the precipitates in chloroform from the di-*n*-butylamine and tri-*n*-butylamine modified samples. In-plane XRD patterns of the layered structures were measured at the beamline of BL-16XU at SPring-8 using 10 keV synchrotron radiation. The incident beam and output angles were 0.1° and −0.2°, respectively. The scanning rate was 0.2°/s. Powder XRD measurements of refined samples filled into glass capillaries were also performed at the same beamline with the same incident photon energy and scanning rate as that for the in-plane measurement.

Photoluminescence and Photoluminescence Excitation (PL and PLE). PL and PLE spectra were obtained using a Jasco FP-6500ST spectrofluorometer with 0.1% chloroform solutions of the refined samples in quartz cells. The excitation wavelength was 350 nm for the PL measurement, and the fluorescence wavelength was 450 nm for the PLE measurement.

UV−Visible Absorption Spectra (UV−vis). UV−vis spectra were measured using a quartz cell with a light path length of 1 cm

on a Shimadzu UV-2100 spectrophotometer (200−800 nm). A stock solution containing 36 mg of the refined C10−Si_n in 20 mL of chloroform was prepared and then diluted to specific concentrations before the measurements. The absorption of the solvent was simultaneously subtracted from each spectrum.

Calculation of Optimal Structure of Si Sheet with Si−NH−R and Si−NR−Si Linkage. To confirm the assumed structural changes of the Si nanosheet corresponding to Si−NR−Si bond creation, theoretical calculations employing quantum chemical methods were performed as follows. First, the Si nanosheet was modeled as Si_{24}. One or two NR (R = CH_3 in the calculations) groups were then introduced onto Si_{24} with substitution of neighboring hydrogen atoms at axial positions. Geometry optimizations were performed using density functional theory (DFT) with the B3LYP hybrid exchange-correlation functional.[33] The basis set used was Pople's 6-31G(d).[34] Calculations were carried out using the Gaussian 03 program package.[35]

Acknowledgment. This work was supported by Grant-in-Aid for Scientific Research (19350105).

Supporting Information Available: Additional XANES spectra measured using the FY mode and a complete ref 35. This material is available free of charge via the Internet at http://pubs.acs.org.

JA908827Z

(33) (a) Becke, A. D. *J. Chem. Phys.* **1993**, *98*, 5648–5652. (b) Lee, C.; Yan, W. R.; Parr, R. G. *Phys. Rev. B* **1988**, *37*, 785–789.

(34) (a) Hehre, W. J.; Ditchfield, R.; Pople, J. A. *J. Chem. Phys.* **1972**, *56*, 2257–2261. (b) Francl, M. M.; Pietro, W. J.; Hehre, W. J.; Binkley, J. S.; Gordon, M. S.; DeFrees, D. J.; Pople, J. A. *J. Chem. Phys.* **1982**, *77*, 3654–3665.

(35) Frisch, M. J. et al. *Gaussian 03, Revision E.01*, Gaussian Inc.: Wallingford CT, 2004.